Depth-domain velocity analysis in VTI media using surface P-wave data: Is it feasible?

Yves Le Stunff †, Vladimir Grechka⋆, and Ilya Tsvankin⋆

† *Total, Route de Versailles, 78470 St. Remy Les Chevreuse, France*

⋆ *Center for Wave Phenomena, Department of Geophysics, Colorado School of Mines, Golden, CO 80401-1887*

ABSTRACT

The main difficulties in anisotropic velocity analysis and inversion using surface seismic data are associated with the multi-parameter nature of the problem and inherent trade-offs between the model parameters. For the most common anisotropic model, transverse isotropy with a vertical symmetry axis (VTI media), P-wave kinematic signatures are controlled by the vertical velocity V_0 and the anisotropic parameters ϵ and δ. However, only two combinations of these parameters – NMO velocity from a horizontal reflector $V_{\rm nmo}(0)$ and the anellipticity coefficient η – can be determined from P-wave reflection traveltimes if the medium above the reflector is laterally homogeneous. While $V_{\rm nmo}(0)$ and η are sufficient for time-domain imaging in VTI media, they cannot be used to resolve the vertical velocity and build velocity models needed for *depth* migration.

Here, we demonstrate that P-wave reflection data can be inverted for all three relevant VTI parameters (V_0, ϵ and δ) if the model contains *non-horizontal* intermediate interfaces. Using anisotropic reflection tomography, we carry out parameter estimation for a two-layer medium with a curved intermediate interface and reconstruct the correct anisotropic depth model. To show that the success of this inversion procedure was not fortuitous, we present an analytic study of reflection traveltimes for this model and demonstrate that the information about the vertical velocity and reflector depth was contained in the reflected rays which crossed the dipping intermediate interface.

The results of this work are especially encouraging because the need for depth imaging (such as prestack depth migration) arises mostly in laterally heterogeneous media. Still, we restricted this study to a relatively simple model and constrained the inversion by assuming that one of the layers is isotropic. In general, although lateral heterogeneity does create a dependence of P-wave reflection traveltimes on the vertical velocity, there is no guarantee that for more complicated models all anisotropic parameters can be resolved in a unique fashion.

Key words: VTI media, P-wave reflection data, depth-domain velocity analysis

Introduction

To constrain the anisotropic velocity model using surface data it is beneficial to record reflected rays spanning a wide range of propagation directions. The presence of reflectors with different dips or acquisition of long-offset data help to achieve that goal (e.g., Tsvankin and Thomsen, 1995; Alkhalifah and Tsvankin, 1995). Wide-angle recording, however, implies that the rays cover a relatively large subsurface area and may be influenced by lateral heterogeneity in the form of either smooth velocity variations or dip and irregular shape of intermediate interfaces. In general, lateral heterogeneity may significantly complicate the inversion process by introducing additional trade-offs between the model parameters.

(Note that the problem of separating the contribution of lateral velocity variation to reflection traveltimes from that of the shape of interfaces is known to be quite involved even for isotropic media.) It turns out, however, that as long as the subsurface structure and the velocity model remain relatively simple, lateral heterogeneity can actually help in constraining the parameters which are impossible to obtain in similar models with a homogeneous or horizontally layered overburden. This point is illustrated here for a two-layer transversely isotropic medium with a dipping intermediate interface.

Parameter estimation in transversely isotropic media with a vertical axis of symmetry (VTI media) has attracted considerable attention in the literature in the past several years (e.g., Bube and Meadows, 1997; Grechka and Tsvankin, 1998; Bartel et al., 1998; Le Stunff and Grenié, 1998; Le Stunff and Jeannot, 1998; Sexton and Williamson, 1998). One of the common conclusions that can be drawn from these publications is that surface P-wave reflection data in VTI media are inherently insufficient to constrain the vertical velocity and find reflector depth. Analytic support for this result is provided by the work of Alkhalifah and Tsvankin (1995), who showed that P-wave reflection traveltimes are fully controlled by only *two* parameters – the NMO velocity from a horizontal reflector

$$V_{\rm nmo}(0) = V_0\sqrt{1+2\,\delta} \tag{1}$$

and the "anellipticity" coefficient

$$\eta \equiv \frac{\epsilon-\delta}{1+2\,\delta}\,. \tag{2}$$

Here V_0 is the P-wave vertical velocity, and ϵ and δ are Thomsen (1986) anisotropy parameters; V_0, ϵ and δ fully control P-wave kinematic signatures in VTI media (Tsvankin, 1996). Since the vertical velocity contributes to $V_{\rm nmo}(0)$ [equation (1)] only in combination with δ, it seems that P-wave traveltime data cannot be used to resolve V_0 and constrain the depth scale in VTI media. As a result, one has to rely on additional information (e.g., borehole data) in building anisotropic velocity models for prestack and poststack depth migration.

Alkhalifah-Tsvankin (1995) result, however, was derived for *laterally-homogeneous* VTI media above a dipping reflector. The presence of lateral heterogeneity in the subsurface may, in principle, cause dependence of P-wave reflection traveltimes on the individual values of V_0, ϵ, and δ. Such a dependence was indeed observed by Alkhalifah et al. (1998), who commented, however, that it was rather weak for the models they tested. Grechka and Tsvankin (1999) demonstrated that P-wave NMO velocities from reflectors beneath layered VTI media with *non-horizontal* intermediate interfaces may contain information about the layers' thicknesses. They emphasized that it is the presence of lateral heterogeneity above the reflector (i.e., the dip of intermediate interfaces) that makes P-wave reflection data dependent on all three Thomsen parameters (V_0, ϵ and δ). Hence, an important practical issue is whether for a certain class of laterally heterogeneous VTI models the parameters V_0, ϵ and δ can be determined unambiguously from surface P-wave data.

Without attempting to answer this question in full generality, we present a successful synthetic example of P-wave reflection tomography in a layered VTI model with a curved intermediate interface. Our results prove that P-wave reflection traveltimes in some piecewise homogeneous VTI models can indeed be inverted for the parameters V_0, ϵ and δ, along with the depths and dips of the reflecting interfaces. This demonstrates the principal feasibility of *depth* processing in VTI media based solely on P-wave reflection data. We begin with a description of our numerical test and then discuss the theory that helps to explain the numerical results.

Tomographic inversion for a two-layer model

The model chosen for tomographic parameter estimation is shown in Figure 1. It contains two homogeneous layers (VTI and isotropic) separated by a curved interface. The traveltimes of P-waves reflected from both interfaces were calculated by ray tracing; acquisition parameters are given in Table 1.

We added Gaussian noise with zero mean and standard deviation 2.5 ms to the traveltimes to simulate picking errors and applied a tomographic algorithm (e.g., Stork and Clayton, 1985; Kaculini and Guiziou, 1992) to perform traveltime inversion. The initial model was purely isotropic with the parameters estimated from conventional time-to-depth conversion. The tomographic procedure updates the model to minimize the misfit between the input and computed traveltimes using a linearized least-squares algorithm (Tarantola, 1987). We constrained the inversion assuming that

(i) the model consists of two homogeneous layers;
(ii) the bottom layer is isotropic;
(iii) the bottom reflector is horizontal.

The intermediate interface was parameterized by a B-spline with 12 nodes (one node per every 40 common midpoints). The model parameters include the vertical velocity $V_{\rm t}$ (the subscript "t" stands for "top") and the coefficients $\epsilon_{\rm t}$ and $\delta_{\rm t}$ in the VTI layer, the velocity $V_{\rm b}$ ("b" stands for "bottom") in the isotropic layer, the depth $Z_{\rm r}$ of the horizontal reflector, and the spline coefficients responsible for the shape and position of the intermediate interface. At each iteration all parameters were

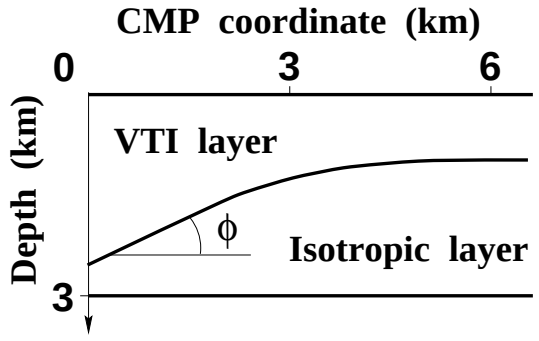

Figure 1. The model used for tomographic parameter estimation. The top layer is VTI with the P-wave vertical velocity $V_{\rm t} = 2.5$ km/s and anisotropic coefficients $\epsilon_{\rm t} = 0.2$ and $\delta_{\rm t} = 0.05$. The bottom layer is isotropic with the P-wave velocity $V_{\rm b} = 3.5$ km/s. The intermediate interface is dipping in the left section of the model (dip $\phi = 25°$ at the zero CMP coordinate) and horizontal on the right. The bottom reflector is horizontal; its depth $Z_{\rm r} = 3$ km.

Number of common midpoints	500
CMP spacing	12.5 m
Number of receivers per CMP gather	40
Receiver spacing	100 m
Minimum offset	0 m
Maximum offset	4000 m

Table 1. Acquisition parameters used in ray tracing. The number of receivers per CMP gather and the maximum offset were reduced for CMP location near the edges of the model.

updated simultaneously. As shown in Figure 2, the algorithm successfully converges towards the correct solution after only a few iterations. Note that since we determined both velocities $V_{\rm t}$ and $V_{\rm b}$, we can reconstruct the actual depths and dips of both interfaces. Clearly, in this example P-wave reflection traveltimes provide enough information for building a model for *depth* imaging.

It may seem that the results of our tomographic experiment contradict the theory of Alkhalifah and Tsvankin (1995), as well as the conclusions of some recent publications cited above. For instance, Bube and Meadows (1997) state that in TI media "... the well-known velocity-depth ambiguity cannot be separated as it can be done in the isotropic case." Indeed, velocity-depth ambiguity in our model cannot be overcome using the reflection from the intermediate interface that yields only the parameters $V_{\rm nmo,t}(0)$ and $\eta_{\rm t}$ in the VTI layer [see equations (1) and (2)] (Alkhalifah and Tsvankin, 1995). Including the reflection from the bottom interface near the right edge of the model (where both interfaces are horizontal, Figure 1), one can also determine the velocity $V_{\rm b}$ in the isotropic layer from the conventional Dix equation. The quantities $V_{\rm nmo,t}(0)$ and $\eta_{\rm t}$, however, provide sufficient information only for time processing and do not constrain the thickness of the VTI layer.

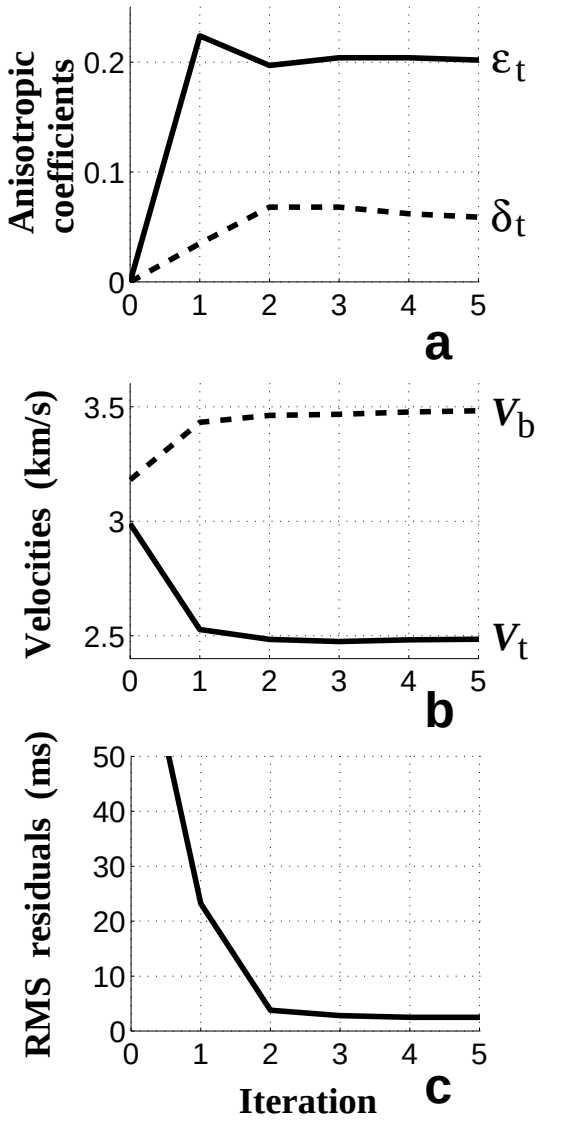

Figure 2. The model parameters and time residuals obtained by the iterative inversion algorithm. (a) Anisotropic coefficients $\epsilon_{\rm t}$ and $\delta_{\rm t}$; (b) the velocities $V_{\rm t}$ and $V_{\rm b}$, and (c) rms traveltime residuals. The residuals at 4th and 5th iterations are equal to the standard deviation of the noise (2.5 ms) added to the data.

Below, we show that the success of the tomographic inversion procedure was ensured by the traveltimes from the bottom reflector near the left edge of the model, where the bottom of the VTI layer is *dipping*. The dip of the intermediate interface causes the dependence of P-wave moveout on all four relevant parameters ($V_{\rm t}$, and $V_{\rm b}$, $\epsilon_{\rm t}$, and $\delta_{\rm t}$), thus constraining the depth scale of the model.

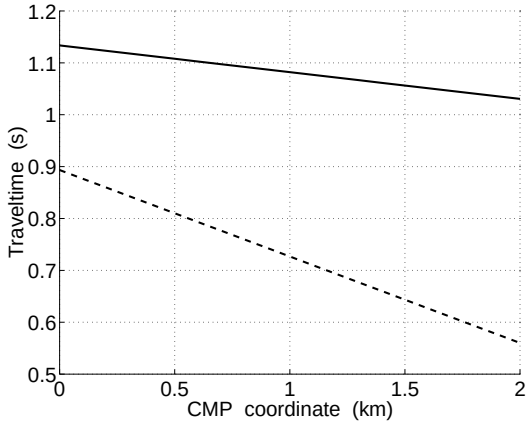

Figure 3. One-way zero-offset traveltimes of the events reflected from the bottom horizontal interface (solid line) and intermediate dipping interface (dashed) on the left-hand side of the model (Figure 1). The slopes of these events (p and p_t, respectively) can be used to constrain the vertical velocity V_t in the top (VTI) layer.

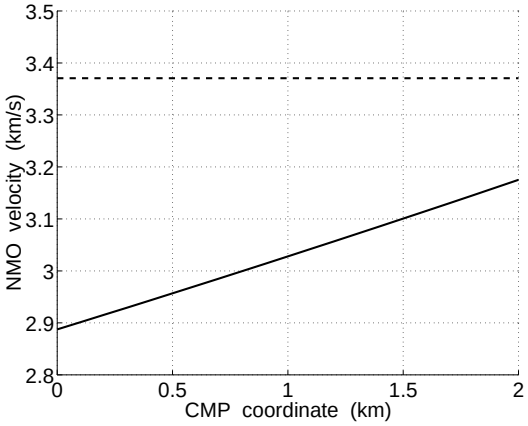

Figure 4. Normal-moveout velocities $V_{nmo}(p)$ from the bottom horizontal reflector (solid line) and $V_{nmo,t}(p_t)$ from the intermediate dipping interface (dashed) near the left edge of the model in Figure 1 where the dip of the intermediate interface is constant.

Analytic explanation of the inversion results

Slopes of the zero-offset reflections

In the dip-moveout inversion algorithm of Alkhalifah and Tsvankin (1995), the slopes of reflection events are supposed to be determined from the zero-offset time section and used as the arguments of the NMO-velocity function. As mentioned above, the DMO inversion in the VTI layer yields the values of the zero-dip NMO velocity $V_{nmo,t}(0)$ and η_t, but not the true vertical velocity. The dip of the intermediate interface, however, also creates a dependence of the slope of the bottom reflection (p) on the parameters of the top (VTI) layer.

As shown in Appendix A, the value of p combined with the slope p_t of the reflection from the intermediate dipping interface (Figure 3) can be used to infer the vertical velocity V_t. Under the assumption of weak anisotropy and mild dip of the intermediate interface, the relation between the two slopes is given by [equation (A6)]

$$p\,V_b \approx p_t\,(V_b - V_t)\,. \qquad (3)$$

Since the velocity V_b in the isotropic layer can be obtained using the Dix differentiation near the right edge of the model (see above), equation (3) yields the velocity V_t. Approximation (3) proved to be reasonably accurate for our model. Indeed, calculating V_t directly from equation (3) yields $V_t = 2.42$ km/s instead of the correct value $V_t = 2.5$ km/s. Then, since the zero-dip NMO velocity $V_{nmo,t}(0)$ can be determined from moveout analysis on the right-hand side of the model, we can use equation (1) to obtain the anisotropic coefficient δ_t ($V_t = 2.42$ km/s gives $\delta_t = 0.04$; the correct value is 0.05). Note that if the intermediate interface is horizontal, $p = p_t = 0$, and equation (3) contains no information about the velocities.

NMO velocity from the bottom reflector

Although, as discussed above, the zero-offset reflection slopes are already sufficient for resolving the vertical velocity in the VTI layer for the whole model, here we show that additional information about V_t is provided by the NMO velocity of the bottom reflection event on the left-hand side of the model. As before, we assume that the zero-dip NMO velocity $V_{nmo,t}(0)$ and η_t were determined using the NMO velocity $V_{nmo,t}(p_t)$ from the intermediate interface (dashed line in Figure 4) and the data from the right-hand side of the model. Then the NMO velocity $V_{nmo}(p)$ from the bottom horizontal reflector on the left-hand side of the model (solid line in Figure 4) can be inverted for the coefficient δ_t and, therefore, the vertical velocity V_t in the VTI layer.

To prove that NMO velocity of the reflection that crosses the dipping intermediate interface depends on the individual values of Thomsen parameters, we use the analytic description of normal-moveout velocity in heterogeneous anisotropic media introduced in Grechka and Tsvankin (1999). Two results of their work applicable to our problem can be briefly summarized as follows:

(i) Normal-moveout velocity of any pure-mode reflection plotted from the common midpoint along all possible directions of CMP lines in 3-D space forms a quadratic "NMO surface," which usually is either a one-sheeted hyperboloid, or a cylinder, or an ellipsoid. If the medium at the common midpoint is locally homo-

geneous, the NMO surface has to be a cylinder. The axis of the NMO cylinder is parallel to the zero-offset ray at the CMP location.

(ii) Dix-type averaging and differentiation procedures are applicable to the cross-sections of the NMO surfaces by planes in which the projections of the slowness vector are locally preserved along the zero-offset ray. Whenever the zero-offset ray intersects a medium interface, the plane of the cross-section is tangent to the interface due to Snell's law.

Here, we discuss a 2-D version of the Grechka-Tsvankin's (1999) Dix-type averaging procedure that is adequate for our test model (Figure 1). Since both layers are homogeneous and the model is two-dimensional, the NMO surfaces of all reflections are cylinders with the axes confined to the vertical incidence plane. Cross-sections of these cylinders by the interfaces will represent ellipses (or circles in special cases) with the axes in the incidence plane and orthogonal to it. Since in our tomographic experiment we did not measure traveltimes outside the incidence plane, we apply the averaging scheme of Grechka and Tsvankin just to the in-plane axes of the cross-sections.

Figure 5 illustrates the process of building the "effective" NMO velocity $V_{\rm nmo}$ for the reflection from the bottom interface on the left-hand side of our model (the intermediate interface is assumed to be plane). $V_{\rm nmo,b}$ and $V_{\rm nmo,t}$ (gray lines in Figures 5a and 5b) are the axes (or semi-axes) of the cross-sections of two interval NMO cylinders (dashed lines in Figures 5a and 5b) by the intermediate interface. Following Grechka and Tsvankin (1999), these axes have to be averaged according to the Dix (1955) formula,

$$V^2_{\rm nmo,s} = \frac{\tau_{\rm b}\, V^2_{\rm nmo,b} + \tau_{\rm t}\, V^2_{\rm nmo,t}}{\tau_{\rm b} + \tau_{\rm t}}, \qquad (4)$$

where $\tau_{\rm b}$ and $\tau_{\rm t}$ are the zero-offset traveltimes in the bottom and top layers (Figure 5a and 5b). This operation yields $V_{\rm nmo,s}$ – the "effective" NMO velocity in the direction parallel to the intermediate interface (gray line in Figure 5c). Finally, the NMO velocity $V_{\rm nmo}(p)$ (Figure 5d) on a surface CMP line is found by projecting $V_{\rm nmo,s}$ along the axes of the NMO cylinder (dashed lines in Figure 5d) onto the horizontal plane.

As shown in Appendix B, the result of this averaging operation can be written as

$$V^2_{\rm nmo}(p) = \frac{V_{\rm b}^2\,(1 - q'\tan\phi)^2}{1 + \tau_{\rm t}/\tau_{\rm b}} + \frac{V^2_{\rm nmo,t}(p)}{1 + \tau_{\rm b}/\tau_{\rm t}}, \qquad (5)$$

where p, as above, is the slope of the reflection from the horizontal interface on the zero-offset section (i.e., the horizontal component of the slowness vector of the zero-offset ray), $q' \equiv dq/dp$ is the derivative of the vertical slowness component q with respect to p, and $V_{\rm nmo,t}(p)$ is the NMO velocity of the reflection from the bottom of the VTI layer corresponding to the same value of p.

Next, we analyze equation (5) to show that the NMO velocity $V_{\rm nmo}(p)$ depends on $\delta_{\rm t}$ for given values of $V_{\rm nmo,t}(0)$ and $\eta_{\rm t}$. Note that the normal-moveout velocity $V_{\rm nmo,t}(p)$ in the numerator of the second term is a function of just p, $\eta_{\rm t}$ and $V_{\rm nmo,t}(0)$, with no separate dependence on $\delta_{\rm t}$ (Alkhalifah and Tsvankin, 1995). In contrast, $\delta_{\rm t}$ does contribute to the numerator of the first term through the product $q'\tan\phi$. The simplest way to demonstrate that $q'\tan\phi$ is indeed a function of $\delta_{\rm t}$ is to obtain its approximation in the weak anisotropy limit [equation (B8) in Appendix B]:

$$q'\tan\phi \approx V_{\rm b}\,[p\,V_{\rm nmo,t}(0)]^2\;\frac{V_{\rm nmo,t}(0)\,(1+\delta_{\rm t}) - V_{\rm b}}{[V_{\rm nmo,t}(0) - V_{\rm b}]^2}. \qquad (6)$$

It can be shown that $\delta_{\rm t}$ also influences the ratio of the traveltimes in the two layers ($\tau_{\rm t}/\tau_{\rm b}$). This ratio, unlike the term $q'\tan\phi$, changes with the CMP coordinate $X_{\rm CMP}$, which makes $V_{\rm nmo}(p)$ from equation (5) a laterally varying function as well (Figure 4). From the structure of equation (5) and the fact that $q'\tan\phi$ is not a function of $X_{\rm CMP}$, it is clear that the dependence of $q'\tan\phi$ on $\delta_{\rm t}$ cannot be compensated by the traveltime ratio $\tau_{\rm t}/\tau_{\rm b}$ for all CMP locations.

We conclude that the NMO velocity $V_{\rm nmo}(p)$ as a whole depends on the anisotropic parameter $\delta_{\rm t}$ in addition to $V_{\rm nmo,t}(0)$ and $\eta_{\rm t}$. According to equation (5), our ability to invert the NMO velocity of the bottom event for the parameter $\delta_{\rm t}$ and, consequently, for the depth of the intermediate interface is tied to the interface dip ϕ. The greater the dip, the better $\delta_{\rm t}$ and the vertical velocity $V_{\rm t}$ are constrained by the reflection traveltimes. If the intermediate interface is horizontal, $V_{\rm nmo}(p=0)$ is completely independent of $\delta_{\rm t}$ because $q'\tan\phi = 0$, and the traveltime ratio $\tau_{\rm t}/\tau_{\rm b}$ is determined only by the vertical velocities.

Inversion on the left-hand side of the model

Our analytic results show that the presence of the dipping intermediate interface plays a crucial role in constraining the vertical velocity $V_{\rm t}$ in the VTI layer. In the discussion above, however, we assumed that the velocities $V_{\rm nmo,t}(0)$ and $V_{\rm b}$ were obtained from moveout analysis on the right-hand side of the model (Figure 1). Here we demonstrate that this assumption is unnecessary, and it is possible to find all VTI parameters using *only* the traveltimes near the left edge of the model.

Neglecting the curvature of the intermediate interface, the left-hand side of the model can be fully described by the following seven parameters: the dip ϕ and the depth $Z_{\rm i}$ (say, at the zero CMP coordinate

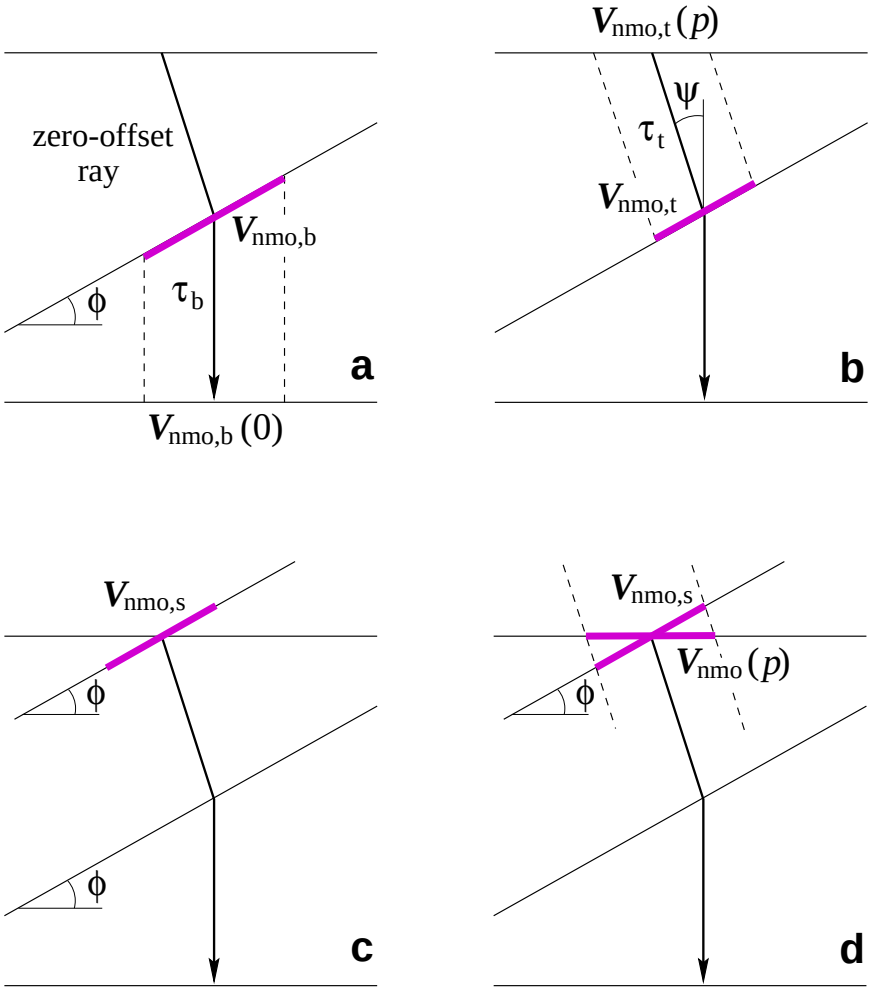

Figure 5. 2-D version of the Dix-type averaging procedure (Grechka and Tsvankin, 1999) for a two-layer model with an intermediate dipping interface. $V_{\rm nmo,b}$ (a) and $V_{\rm nmo,t}$ (b) are the in-plane axes of the cross-sections of the interval NMO cylinders in the isotropic and VTI layers. Dix averaging of $V_{\rm nmo,b}$ and $V_{\rm nmo,t}$ produces the in-plane axis $V_{\rm nmo,s}$ (c) of the cross-section of the "effective" NMO cylinder. $V_{\rm nmo,s}$ is then projected along the NMO cylinder onto the horizontal plane yielding the NMO velocity $V_{\rm nmo}(p)$ (d) measured at the surface.

$X_{\rm CMP}=0$) of the intermediate interface; the depth $Z_{\rm r}$ of the horizontal reflector; the parameters $V_{\rm t}$, $\epsilon_{\rm t}$, and $\delta_{\rm t}$ which control P-wave kinematics in the VTI layer; and the velocity $V_{\rm b}$ in the bottom isotropic layer. As illustrated by Figures 3 and 4, surface data may contain enough information to resolve all these parameters. The zero-offset traveltimes in Figure 3 are linear functions of the CMP coordinate $X_{\rm CMP}$ and, therefore, provide a total of four constraints (i.e., four equations for the unknown parameters). The NMO velocity $V_{\rm nmo,t}(p_{\rm t})$ from the dipping interface (Figure 4) does not depend on $X_{\rm CMP}$, thus adding one more equation. Two more equations come from the NMO velocity $V_{\rm nmo}(p)$ of the bottom event (Figure 4) that depends almost linearly on $X_{\rm CMP}$.

Thus, the traveltime data on the left-hand side of the model yield seven nonlinear equations for seven unknown parameters. We have solved these equations by the simplex method (adding Gaussian noise with the standard deviation 2.5 ms to the traveltimes) and obtained accurate estimates of the model parameters close to those determined from reflection tomography (Figure 2).

Possible trade-offs in the estimated parameters

Although we succeeded in using reflection tomography for depth-domain parameter estimation in a two-layer VTI model and corroborated the obtained results theoretically, the unique solution may no longer exist if the model becomes more complicated. For instance, if the bottom layer becomes anisotropic (VTI), the traveltimes on the left-hand side of the model are no longer sufficient

for recovering the vertical velocities. Indeed, the number of available equations remains the same (seven; see the previous section) but the number of unknowns increases due to the addition of the anisotropic coefficients in the bottom layer.

As long as the lower layer is isotropic and homogeneous, we can allow the bottom of the model to have an irregular shape. In fact, a non-horizontal bottom interface may help in the parameter estimation because the reflected rays will sample a wider range of propagation directions in both layers. However, making the bottom layer anisotropic, generally creates the trade-off between the anisotropic parameters and the depth and shape of the bottom reflector.

Lateral velocity variation can further complicate the trade-offs between the reflector shape/position and anisotropy (e.g., Grechka and McMechan, 1997). Although one may hope to resolve these trade-offs in some special cases, the separation of lateral heterogeneity from the structural factor cannot be achieved even in general isotropic media, if the input data are limited to the zero-offset traveltimes and NMO velocities (Goldin, 1986).

Discussion and conclusions

Lateral heterogeneity is commonly perceived as one of the main hindrances in velocity analysis and parameter estimation, especially if the medium is anisotropic. For example, it is known that the interplay between anisotropy and lateral velocity variation can substantially hamper our ability to determine the anisotropic parameters of VTI media (Grechka, 1998). Therefore, it is not surprising that parameter estimation in VTI media has been largely based on the theory by Alkhalifah and Tsvankin (1995) developed for *laterally homogeneous* overburden above a horizontal or dipping reflector. The results of Alkhalifah and Tsvankin clearly show that P-wave reflection traveltimes in such a model are fully controlled by the vertical traveltime and just two parameters – the zero-dip NMO velocity $V_{\rm nmo}(0)$ and the anisotropic coefficient η. Both parameters can be obtained by inverting either dip-dependent NMO velocity or non-hyperbolic (long-spread) moveout and can be used for anisotropic *time* processing (NMO, DMO, time migration). While the extension of time-domain velocity analysis and imaging to VTI media produced a number of impressive results (such as superior imaging of dipping reflectors), the problem of building anisotropic models for depth imaging without using additional information (e.g., borehole data or PS-waves) remained unresolved.

This work demonstrates that for certain types of *laterally heterogeneous* VTI media it may be feasible to invert P-wave moveout for all three relevant Thomsen parameters (the vertical velocity V_0 and the anisotropic coefficients ϵ and δ) and, therefore, to find the depth-dependent velocity field. Our model included a VTI layer with a curved lower boundary overlying a purely isotropic layer. Analytic expressions for the reflection slopes and NMO velocities show that the information about the vertical velocity and thickness of the VTI layer was contained in the reflection event transmitted through the *dipping* intermediate interface.

Despite the success of our inversion procedure, it is clear that increasing complexity of the model (e.g., lateral velocity gradients) can cause trade-offs between the parameters and ambiguity in the inversion results. Also, the unique solution in our example was achieved by *assuming* that the second layer is isotropic and has a horizontal lower boundary. Evidently, while the dip of intermediate interfaces and possibly some other relatively simple types of lateral heterogeneity may be helpful in anisotropic velocity analysis, the range of laterally heterogeneous VTI models susceptible to the tomographic inversion of reflection traveltimes is rather restricted. The formalism used here to explain the numerical results may be applied in more complicated models to identify the subsets of model parameters constrained by the reflection traveltimes.

Acknowledgments

Y. Le S. thanks J.P. Jeannot and P. Hardy (GX Technology) for their contribution to the tomography software. V.G. and I.T. were partially supported by the members of the Consortium Project on Seismic Inverse Methods for Complex Structures at CWP and by the United States Department of Energy (project "Three-Dimensional Analysis of Seismic Signatures and Characterization of Fluids and Fractures in Anisotropic Formations"). I.T. also acknowledges the Shell Foundation for providing the Shell Faculty Career Initiation Grant.

References

Alkhalifah, T., Biondi, B., and Fomel, S., 1998, Time-domain processing in arbitrary inhomogeneous media: 68th Ann. Internat. Mtg., Soc. Expl. Geophys., Expanded Abstracts, 1756–1759.

Alkhalifah, T., and Tsvankin, I., 1995, Velocity analysis in transversely isotropic media: Geophysics, **60**, 1550–1566.

Bartel, D.C., Abriel, W.L., Meadows, M.A, and Hill, N.R., 1998, Determination of transversely isotropic velocity parameters at the Pluto Discovery, Gulf of Mexico: 68th Ann. Internat. Mtg., Soc. Expl. Geophys., Expanded Abstracts, 1269–1272.

Bube, K.P., and Meadows, M.A., 1997, On the null space in linearized anisotropic surface reflection tomography: 67th Ann. Internat. Mtg., Soc. Expl. Geophys., Expanded Abstracts, 1677–1680.

Dix C.H. 1955, Seismic velocities from surface measurements: Geophysics, **20**, 68–86.

Goldin, S.V., 1986, Seismic traveltime inversion: Soc. Expl. Geophys.

Grechka, V., 1998, Transverse isotropy versus lateral heterogeneity in the inversion of *P*-wave reflection traveltimes: Geophysics, **63**, 204–212.

Grechka, V., and McMechan, G.A., 1997, Analysis of reflection traveltimes in 3-D transversely-isotropic heterogeneous media, Geophysics, **62**, 1884–1895.

Grechka, V., and Tsvankin, I., 1998, 3-D description of normal moveout in anisotropic inhomogeneous media: Geophysics, **63**, 1079-1092.

Grechka, V. and Tsvankin, I., 1999, NMO surfaces and Dix-type formulae in heterogeneous anisotropic media: this volume.

Grechka, V., Tsvankin, I., and Cohen, J.K., 1999, Generalized Dix equation and analytic treatment of normal-moveout velocity for anisotropic media: Geophys. Prosp., in print.

Kaculini, S., and Guiziou, J.L., 1992, Prestack reflection tomography in practice: 62th Ann. Internat. Mtg., Soc. Expl. Geophys., Expanded Abstracts, 1046–1049.

Le Stunff, Y., Jeannot, J.P., 1998, Pre-stack anisotropic depth imaging: 60th EAGE Conference, Extended Abstracts.

Le Stunff, Y., Grenié, D., 1998, Taking into account a priori information in 3D tomography: 68th Ann. Internat. Mtg., Soc. Expl. Geophys., Expanded Abstracts, 1875–1878.

Sexton, P., and Williamson, P., 1998, 3D anisotropic velocity estimation by model-based inversion of prestack traveltimes: 68th Ann. Internat. Mtg., Soc. Expl. Geophys., Expanded Abstracts, 1855–1858.

Stork, C., and Clayton, R.W., 1985, Iterative tomographic and migration reconstruction of seismic images: 55th Ann. Internat. Mtg., Soc. Expl. Geophys., Expanded Abstracts, 610–613.

Tarantola, A., 1987, Inverse Problem Theory: Methods for data fitting and model parameter estimation: Elsevier, Amsterdam.

Thomsen, L., 1986, Weak elastic anisotropy: Geophysics, **51**, 1954–1966.

Tsvankin, I., 1996, P-wave signatures and notation for transversely isotropic media: An overview: Geophysics, **61**, 467–483.

Tsvankin, I., and Thomsen, L., 1995, Inversion of reflection traveltimes for transverse isotropy: Geophysics, **60**, 1095-1107.

APPENDIX A: Slopes of the reflection events in the tomographic model

Here we find an approximate relation between the slopes of the zero-offset reflections from the bottom and intermediate interfaces in the model from Figure 1. To simplify the derivation, we assume that the anisotropy in the VTI layer is weak and the dip of the interface is mild.

The zero-offset ray reflected from the bottom of the model is vertical (i.e., perpendicular to the reflector) in the isotropic layer and becomes oblique in the upper (VTI) layer. The horizontal slowness component of this ray at the surface (denoted as p) determines the slope of the bottom reflection on the zero-offset time section. Applying Snell's law at the intermediate interface yields an expression that involves p and the interface dip ϕ:

$$p + \tan\phi \left[\frac{1}{V_{\rm b}} - q\right] = 0\,, \tag{A1}$$

where $V_{\rm b}$ is the velocity in the bottom layer and q is the vertical slowness component of the zero-offset ray in the VTI layer.

Using the weak-anisotropy version of the Christoffel equation, we obtain the following expression for q linearized in the anisotropic parameters $\delta_{\rm t}$ and $\eta_{\rm t}$:

$$q = \frac{(1+\delta_{\rm t})\,(1-y) - \eta_{\rm t}\, y^2}{V_{\rm nmo,t}(0)\,\sqrt{1-y}}\,, \tag{A2}$$

where $V_{\rm nmo,t}(0)$ is the zero-dip NMO velocity in the VTI layer and $y \equiv [p\,V_{\rm nmo,t}(0)]^2$. Substituting equation (A2) into equation (A1) and linearizing the result in the anisotropic coefficients yields

$$\tan\phi = p\,\left[\frac{1+\delta_{\rm t}}{V_{\rm nmo,t}(0)} - \frac{1}{V_{\rm b}}\right] + O(p^3)\,. \tag{A3}$$

Cubic and higher powers of p in equation (A3) are not shown explicitly because the corresponding terms should be small for mild dips.

The dip ϕ can be also found using the reflection from the intermediate interface. Since the slowness vector $[p_{\rm t}, q_{\rm t}]$ of the zero-offset reflected ray is orthogonal to the interface,

$$\tan\phi = \frac{p_{\rm t}}{q_{\rm t}}\,. \tag{A4}$$

Combining equations (A2) (where q should be replaced by $q_{\rm t}$ and p by $p_{\rm t}$) and (A4) allows us to express $\tan\phi$ through the slope $p_{\rm t}$:

$$\tan\phi = p_{\rm t}\,V_{\rm nmo,t}(0)\,(1-\delta_{\rm t}) + O(p_{\rm t}^3)\,. \tag{A5}$$

Substituting equation (A3) into (A5) and retaining only linear terms in $p_{\rm t}$ and p leads to the following relation between the slopes of the two reflection events:

$$p \approx p_{\rm t}\,\left[1 - (1-\delta_{\rm t})\,\frac{V_{\rm nmo,t}(0)}{V_{\rm b}}\right] \approx p_{\rm t}\,\left[1 - \frac{V_{\rm t}}{V_{\rm b}}\right]\,, \tag{A6}$$

where V_t is the vertical P-wave velocity in the top VTI layer.

APPENDIX B: NMO velocity for the bottom reflector

The P-wave NMO velocity V_{nmo} for the bottom reflection event (Figure 5) can be found using the general formalism developed by Grechka and Tsvankin (1999). As discussed in the main text, the Dix-type expressions of Grechka and Tsvankin operate with the cross-sections of NMO cylinders by model interfaces. In our 2-D problem, we will need to obtain only the in-plane axes of these cross-sections (i.e., the axes confined to the vertical incidence plane).

First, we have to find the velocities $V_{nmo,b}$ and $V_{nmo,t}$ (gray lines in Figures 5a and 5b), which correspond to the cross-sections of the interval NMO cylinders by the intermediate interface. The NMO cylinder in the bottom layer is circular and oriented vertically (dashed lines in Figure 5a), so its axis is parallel to the vertical segment of the zero-offset ray. The radius of the circle $V_{nmo,b}(0)$ at the bottom of the NMO cylinder is simply equal to the velocity V_b because the bottom layer is isotropic. As illustrated by Figure 5a, the cross-section $V_{nmo,b}$ of the cylinder by the intermediate interface is given by

$$V_{nmo,b} = \frac{V_b}{\cos\phi}\,. \tag{B1}$$

Equation (B1) is the familiar expression for the dip-component of NMO velocity in isotropic media.

The axis of the NMO cylinder in the VTI layer is parallel to the group velocity vector (i.e., to the zero-offset ray; see Figure 5b). The angle ψ between the zero-offset ray and vertical can be written as (Grechka et al., 1999)

$$\tan\psi = -\frac{dq}{dp} \equiv -q'\,, \tag{B2}$$

where p and q are the horizontal and vertical slowness components of the zero-offset ray in the VTI layer. The quantity $V_{nmo,t}(p)$ in Figure 5b corresponds to the dip component of the NMO velocity from a dipping reflector (non-existent in our model) orthogonal to the slowness vector $\{p, q\}$. $V_{nmo,t}(p)$ has to be projected onto the dipping intermediate interface along the axes of the NMO cylinder (the dashed lines in Figure 5b). This projection, denoted by $V_{nmo,t}$, can be determined from the law of sines:

$$V_{nmo,t} = V_{nmo,t}(p)\,\frac{\cos\psi}{\cos(\psi-\phi)}\,. \tag{B3}$$

Substituting $\tan\psi$ from equation (B2) yields

$$V_{nmo,t} = \frac{V_{nmo,t}(p)}{\cos\phi\,(1-q'\tan\phi)}\,. \tag{B4}$$

The second step in our derivation is the Dix averaging of the velocities described by equations (B1) and (B4):

$$V^2_{nmo,s} = \frac{1}{\tau_b+\tau_t}\left[\tau_b\,\frac{V_b^2}{\cos^2\phi} + \tau_t\,\frac{V^2_{nmo,t}(p)}{\cos^2\phi\,(1-q'\tan\phi)^2}\right] \tag{B5}$$

The averaged velocity $V_{nmo,s}$ corresponds to the cross-section of the "effective" NMO cylinder by a plane parallel to the dipping interface (gray line in Figure 5c).

Finally, we project $V_{nmo,s}$ onto the horizontal plane to obtain the NMO velocity $V_{nmo}(p)$ (Figure 5d) of the bottom reflection event that can be measured from surface data. This projection can be obtained directly from equations (B3) and (B4):

$$\begin{aligned} V_{nmo}(p) &= V_{nmo,s}\,\frac{\cos(\psi-\phi)}{\cos\psi} \\ &= V_{nmo,s}\,\cos\phi\,(1-q'\tan\phi)\,. \end{aligned} \tag{B6}$$

Substituting equation (B5) into equation (B6) leads to the final result:

$$V^2_{nmo}(p) = \frac{\tau_b\,V_b^2\,(1-q'\tan\phi)^2 + \tau_t\,V^2_{nmo,t}(p)}{\tau_b+\tau_t}\,. \tag{B7}$$

Equation (B7) is almost identical to the conventional Dix (1955) formula, but it contains the factor $(1-q'\tan\phi)^2$ that appears due to the dip ϕ of the intermediate interface. To gain insight into the dependence of $q'\tan\phi$ on the model parameters, we simplify this expression assuming that the dip ϕ is small (i.e., $|\tan\phi| \ll 1$) and anisotropy is weak (i.e., $|\delta_t| \ll 1$ and $|\eta_t| \ll 1$). The derivative q' can be obtained by differentiating equation (A2), while $\tan\phi$ is given by equation (A3). Keeping only linear terms in the anisotropic coefficients and terms up to quadratic in the slope p, we find

$$q'\tan\phi \approx V_b\,[p\,V_{nmo,t}(0)]^2\,\frac{V_{nmo,t}(0)\,(1+\delta_t)-V_b}{[V_{nmo,t}(0)-V_b]^2}\,. \tag{B8}$$

Clearly, even for weak anisotropy the term $q'\tan\phi$ depends not only on the NMO velocity $V_{nmo,t}(0)$, but also on the anisotropic coefficient δ_t; implications of this result are discussed in the main text.